



Figures and figure supplements

Genomic variations of the mevalonate pathway in prokeratosis

et al

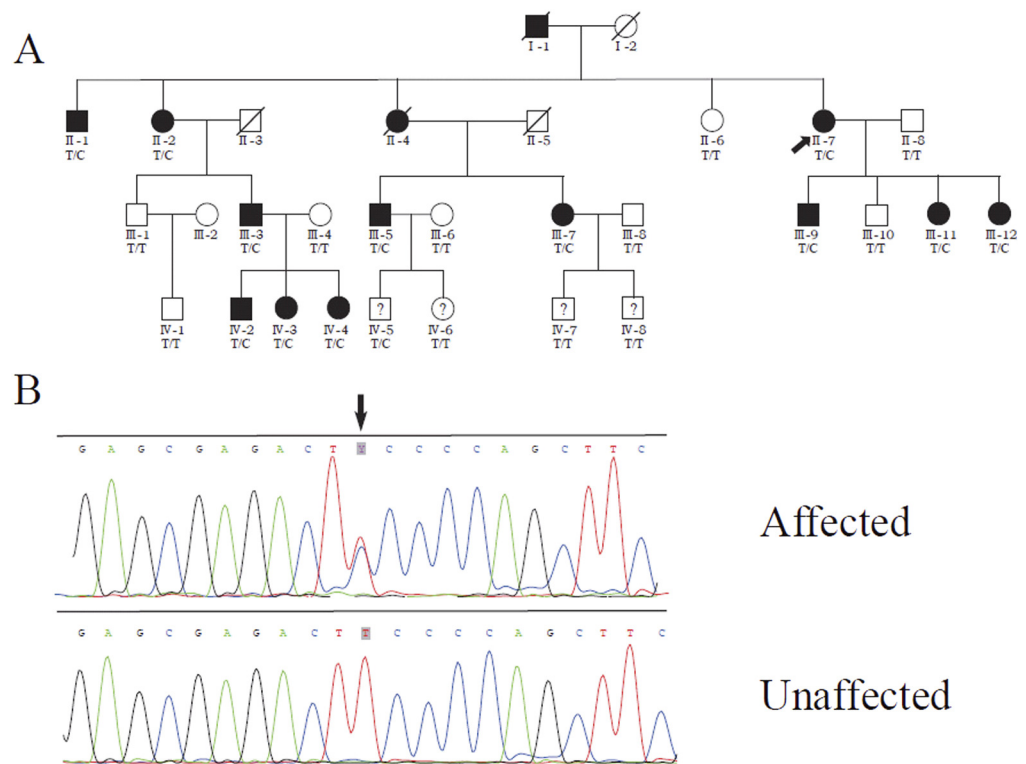
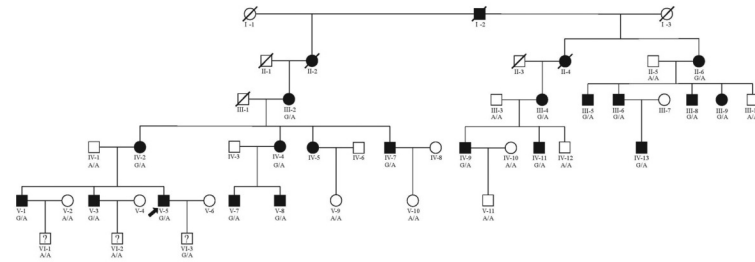


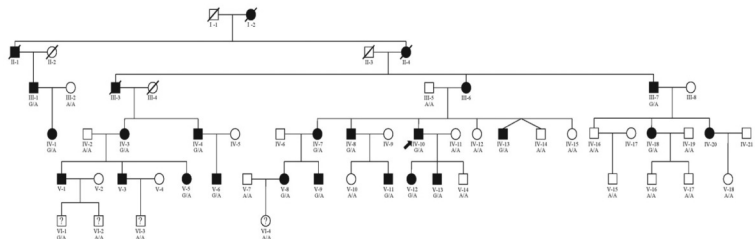
Figure 1. Identification of a *MVD* mutation in a porokeratosis (PK) family. (A) c.746T>C (p.Phe249Ser) in *MVD* displayed 100% co-separation with PK phenotype in this family (Luan *et al.*, 2011). (B) Sanger sequencing chromatograms of proband (II-7, affected) and normal control (II-8, unaffected) at the c.746T>C mutation site indicated by arrow.

DOI: <http://dx.doi.org/10.7554/eLife.06322.003>

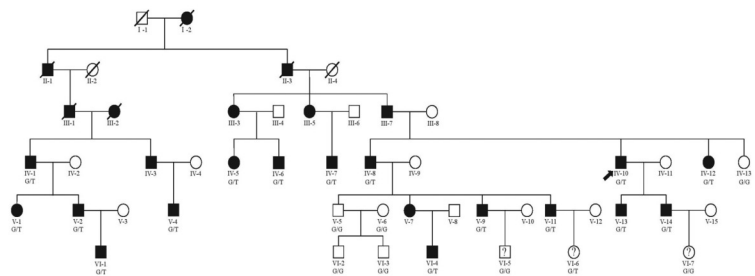
A F-1 with *MVK* mutation (c.935A>G)



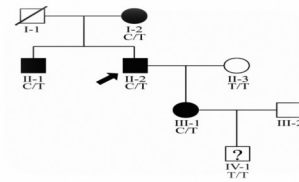
B F-2 with *MVK* mutation (c.1024A>G)



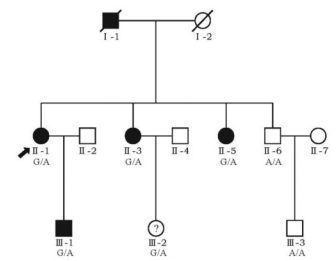
C F-24 with *MVK* mutation (c.74G>T)



D F-5 with *MVD* mutation (c.746T>C)



E F-11 with *MVD* mutation (c.1A>G)



F F-23 with *MVD* mutation (c.1A>G)

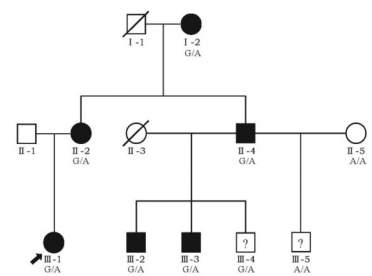


Figure 1—figure supplement 1. Examples of six pedigree charts showing that each mutation displayed 100% co-segregation with the porokeratosis (PK) phenotype in the family.

DOI: <http://dx.doi.org/10.7554/eLife.06322.004>

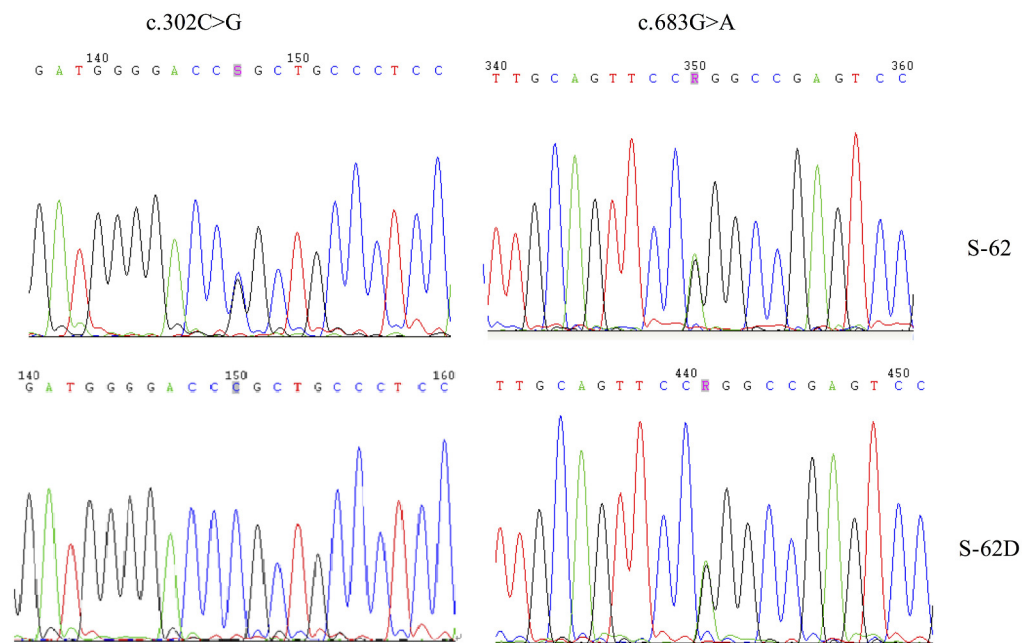


Figure 1—figure supplement 2. Two MVD mutations, c.302C>G (p.Pro101Arg) and c.683 G>A (p.Arg228Gln), for S-62 were located in the trans position because his daughter (S-62-D) carried only one of them.

DOI: <http://dx.doi.org/10.7554/eLife.06322.005>

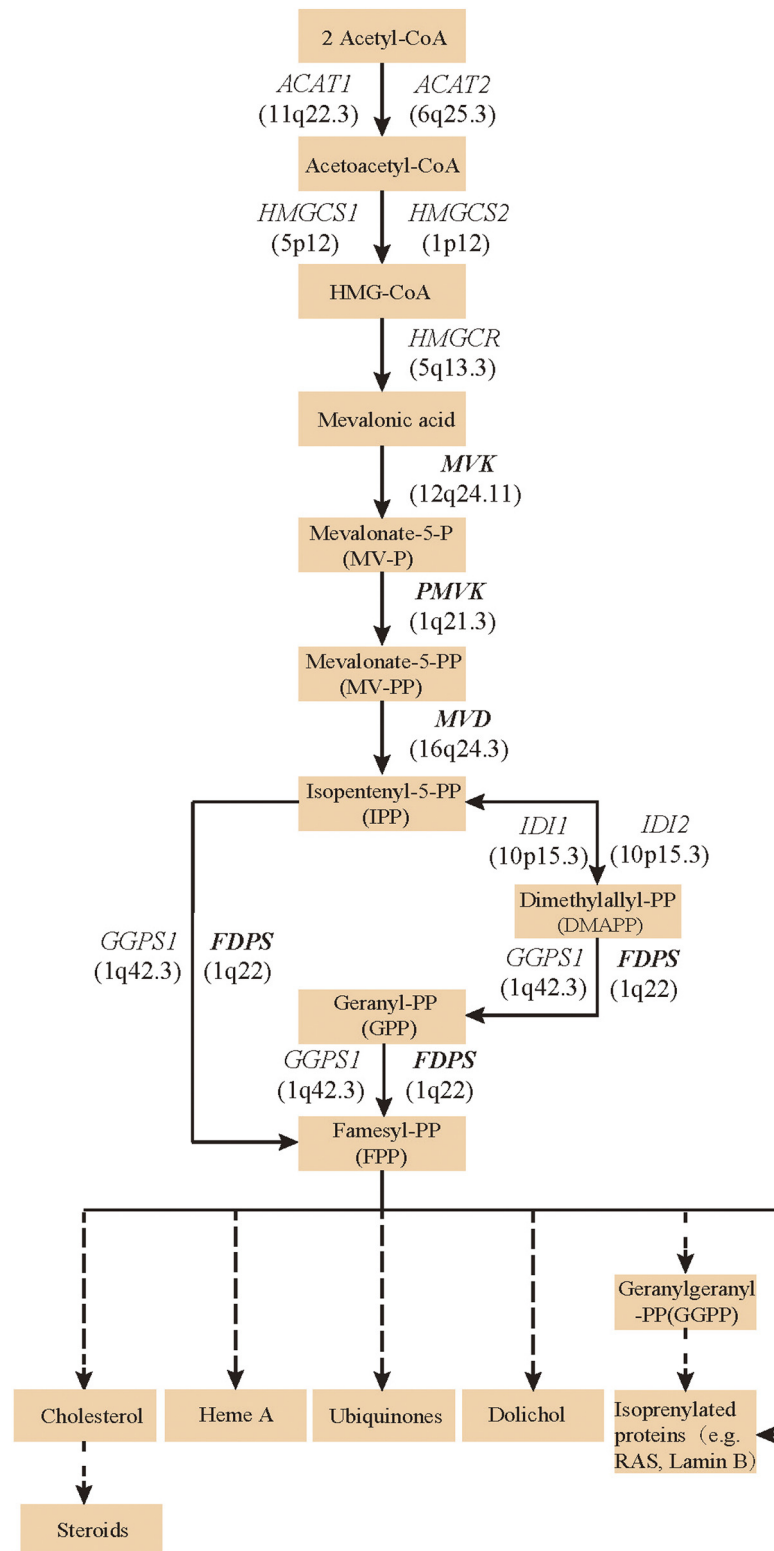
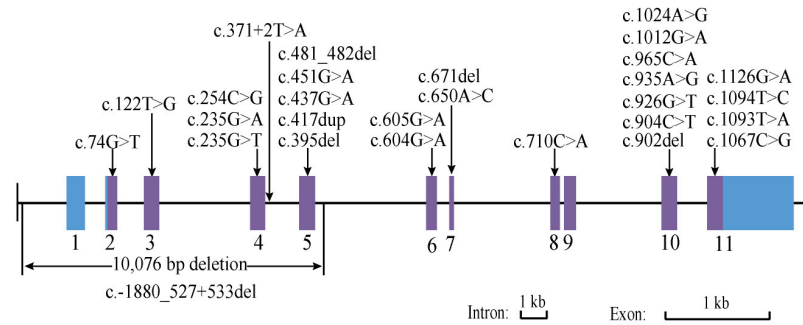


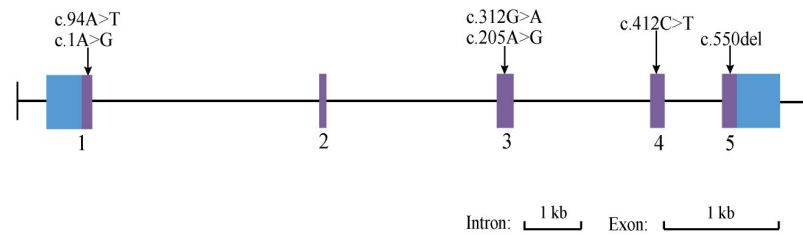
Figure 2. Isoprenoid biosynthesis via the mevalonate pathway. 12 member genes (*ACAT1*, *ACAT2*, *HMGCS1*, *HMGCS2*, *HMGCR*, *MVK*, *PMVK*, *MVD*, *IDI1*, *IDI2*, *FDPS*, *GGPS1*) were subject to mutation screening. The genomic loci of the 12 member genes are provided in parentheses. The illustration is adapted from the 00900 interactive map of the Kyoto Encyclopedia of genes and genomes (KEGG) (*Kanehisa et al., 2012*).

DOI: <http://dx.doi.org/10.7554/eLife.06322.006>

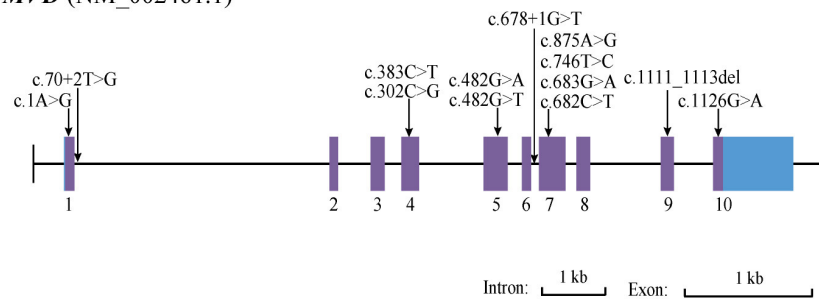
MVK (NM_000431.2)



PMVK (NM_006556.3)



MVD (NM_002461.1)



FDPS (NM_001135822.1)

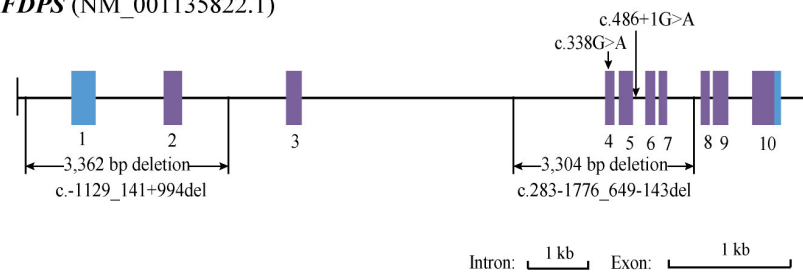


Figure 3. Mutational spectrum of *MVK*, *PMVK*, *MVD* and *FDPS* in 113 of the 134 porokeratosis (PK) patients.

DOI: <http://dx.doi.org/10.7554/eLife.06322.007>

The following source data is available for figure 3:

Source data 1. Sanger sequencing chromatograms of normal control and porokeratosis (PK) patients at 48 mutation sites in *MVK*, *PMVK*, *MVD* and *FDPS*.

DOI: <http://dx.doi.org/10.7554/eLife.06322.008>

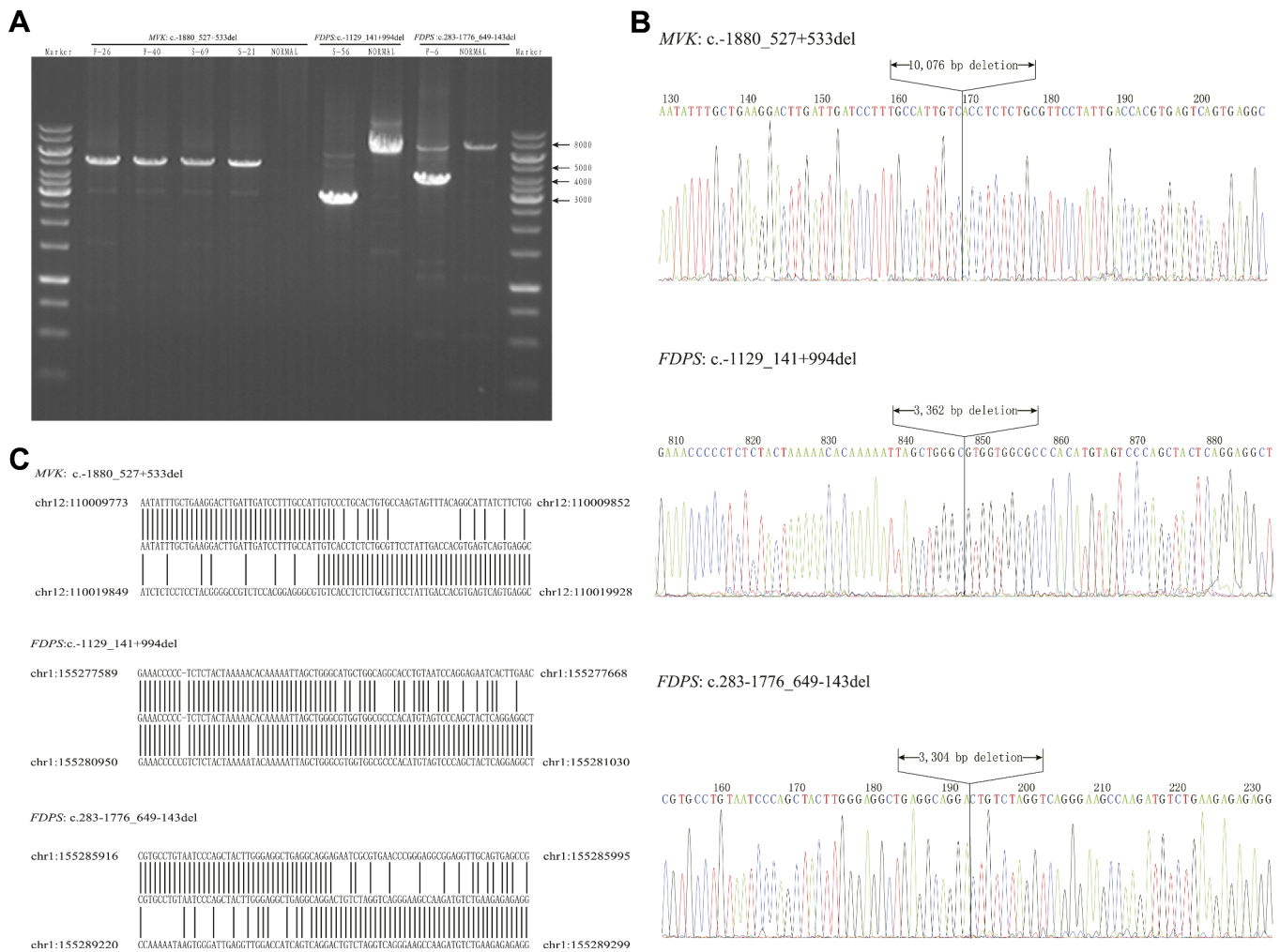


Figure 3—figure supplement 1. Breakpoint analysis for three large deletion mutations in *MVK* and *FDPS* genes. (A) Agarose electrophoresis analysis of long PCR products from patients with deletion mutations and a normal control. (B) Sequencing chromatograms of long PCR products from deletion mutations. (C) Alignment of the sequences from three deletion mutations with human genome reference GRch38 primary assembly indicates a deletion of 10,076 bp, 3362 bp and 3304 bp, respectively.

DOI: <http://dx.doi.org/10.7554/eLife.06322.009>

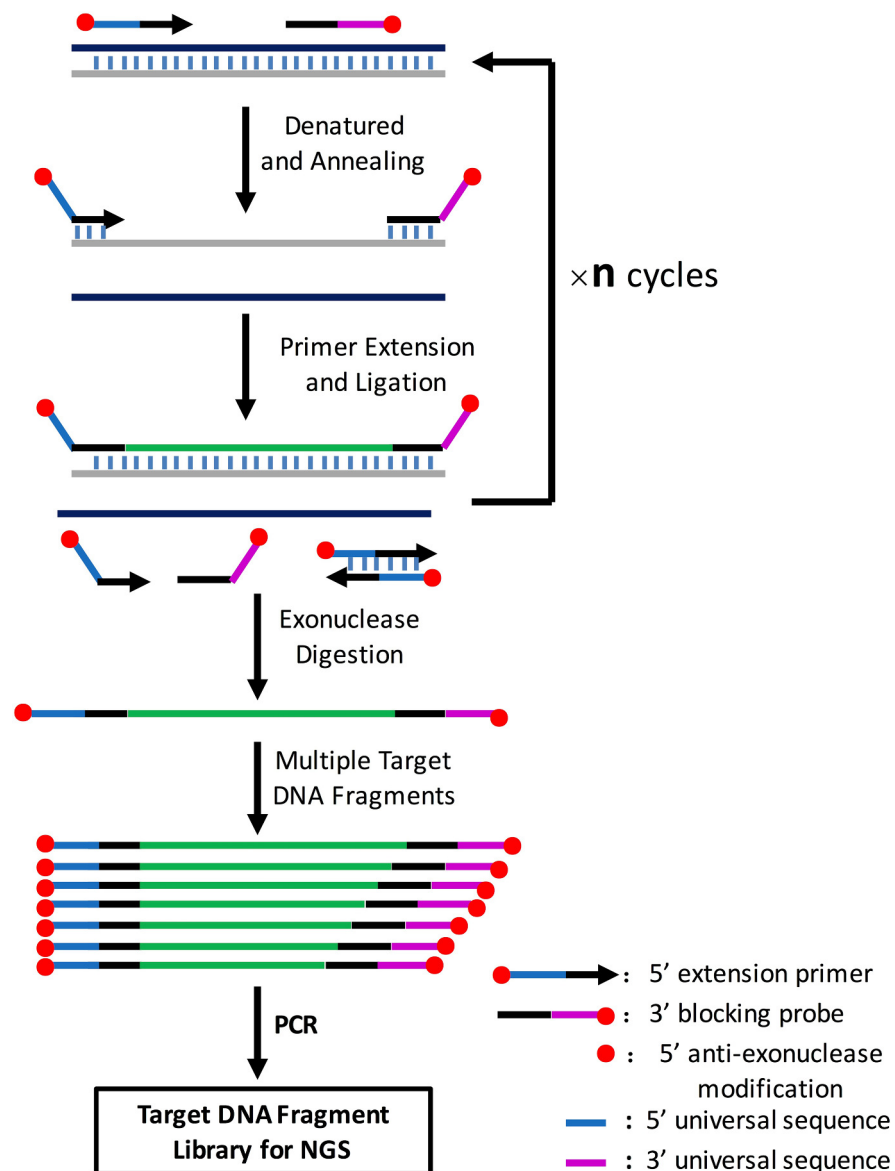


Figure 3—figure supplement 2. Illustration of amplification of multiple target DNA fragments mediated by cycled primer extension and ligation. In brief, for each target region, an extension primer and a block probe are designed. The extension primer has a 5' exonuclease-resistance modification and the block probe has a 5' phosphate and 3' exonuclease-resistance modification. These two oligos are mixed with genomic DNA, heat-denatured, and then annealed to the same strand of the target DNA fragment. The primer extends and stops until it meets the block probe, and the extension product is then ligated with the block probe by a thermal stable ligase. The above procedure can be repeated n times on the PCR machine using a two-step PCR cycling program. The extension and ligation product is then purified by an exonuclease mixture digestion to remove any DNA fragment with no exonuclease-resistance modification at both ends such as remained primers or probes, primer dimers and genomic DNA, and then amplified using universal NGS PCR primer pairs. A CPELA reaction can include hundreds of extension primer-blocking probe sets and simultaneously amplify hundreds of target DNA fragments for subsequent massively parallel sequencing.

DOI: <http://dx.doi.org/10.7554/eLife.06322.010>

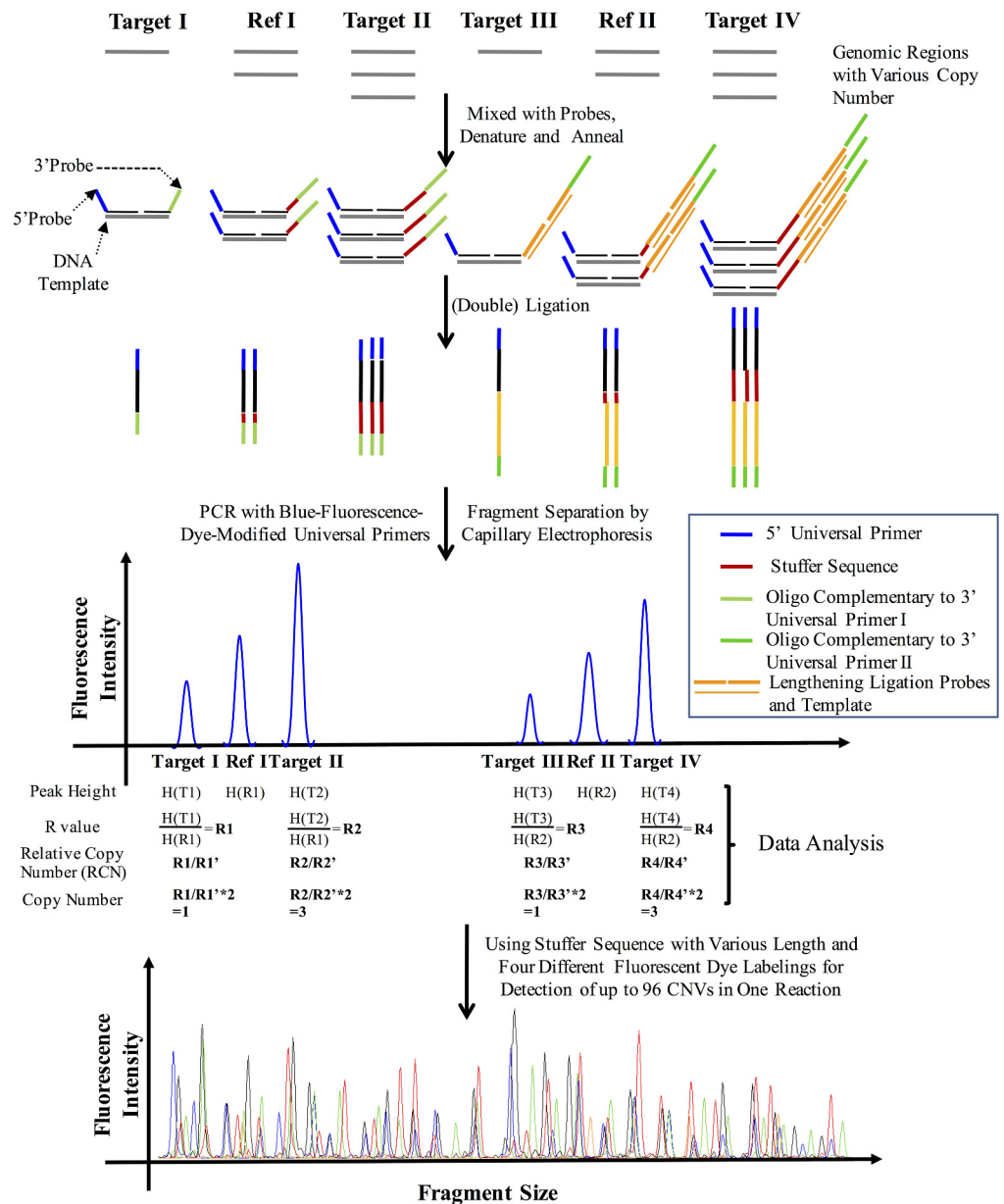


Figure 3—figure supplement 3. The principle of CNVplex technology.
 DOI: <http://dx.doi.org/10.7554/eLife.06322.011>

A From F-42 proband with *MVK* mutation (c.371+2T>A, p.Glu76Glyfs*9)B From F-60 proband with *PMVK* mutation (c.412C>T, p.Arg138*)C From F-36 proband with *MVD* mutation (c.875A>G, p.Asn292Ser)D From F-47 proband with *FDPS* mutation (c.338G>A, p.Arg113Gln)

Figure 4. Representative clinical phenotypes and histopathology associated with the four genotypes. From left to right, pedigree charts, clinical phenotypes and the corresponding histopathology photos are shown correspondingly. (A) Family (F-42) proband with *MVK* mutation showed giant hyperkeratotic plaque-type porokeratosis ptychotopica. (B) F-60 proband with *PMVK* mutation showed tumor-like porokeratoma in the genitogluteal region. (C) F-36 proband with *MVD* mutation showed discrete, red-brown annular keratotic papules or maculopapules on the chest. (D) F-47 proband with *FDPS* mutation showed multiple, small, superficial, annular papules with thread-like ridges on the legs. All histopathology showed cornoid lamella, a histological hallmark of porokeratosis with vertical columns of parakeratosis overlying an area of hypogranulosis with dyskeratotic cells. DOI: <http://dx.doi.org/10.7554/eLife.06322.013>

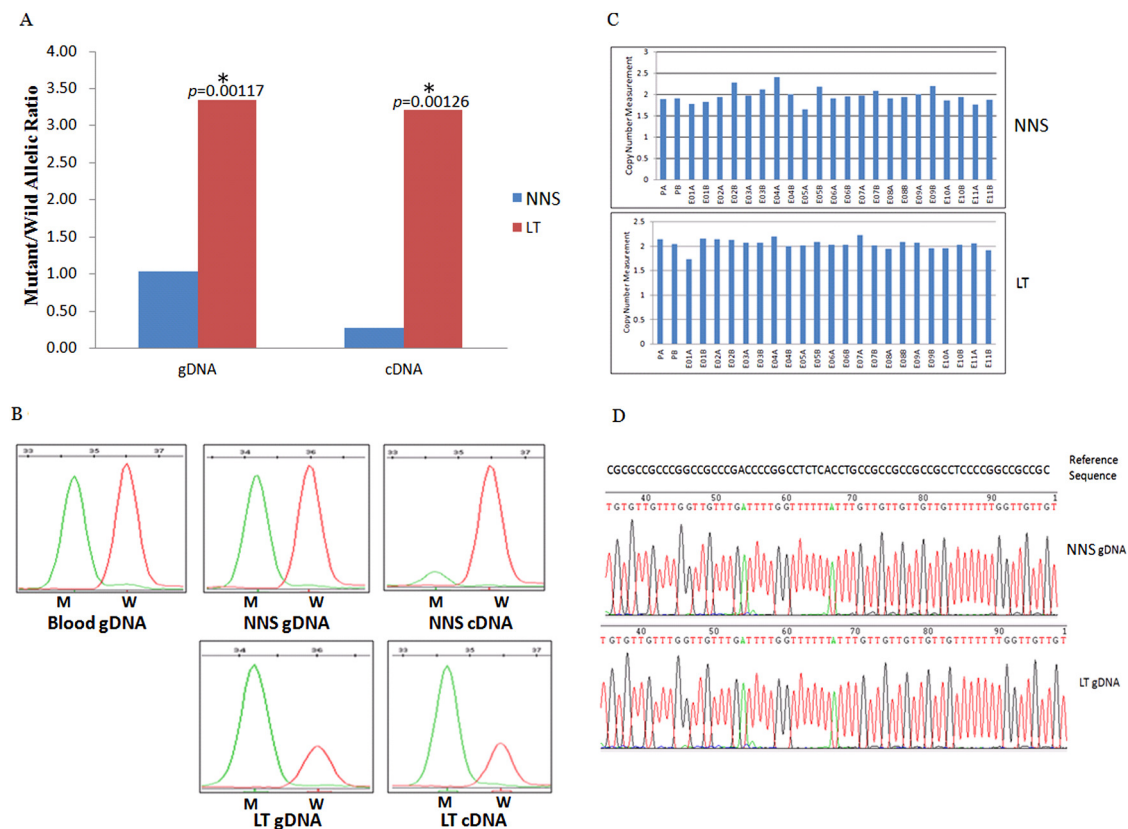


Figure 5. Gene conversion of the wild to mutant allele was identified in a buttock lesion from F-31 carrying a *MVK* mutation of c.395delT. (A) The mutant/wild allelic ratios in genomic DNA (gDNA) and complementary DNA (cDNA) of lesional tissue (LT) and neighboring normal-appearing skin (NNS). The quantity of the mutant allele was about threefold and 10-fold more than the quantity of the wild allele in gDNA and cDNA, respectively. (B) The chromatograms of single nucleotide extension targeting the c.395delT mutation using the SNaPshot kit for five DNA samples (blood gDNA, NNS gDNA, LT gDNA, NNS cDNA and LT cDNA). The mutant peak was overrepresented in both LT gDNA and LT cDNA. (C) No copy number change in genomic DNA of NNS and LT. PA and PB are probes in the promoter region, E01 to E11 designates exon 1 to exon 11, and A or B indicate two different probes in the same exon. (D) The bisulfite sequencing of NNS gDNA and LT gDNA. No methylation was observed for the targeted CpG sites in the promoter region of *MVK*.
DOI: <http://dx.doi.org/10.7554/eLife.06322.014>

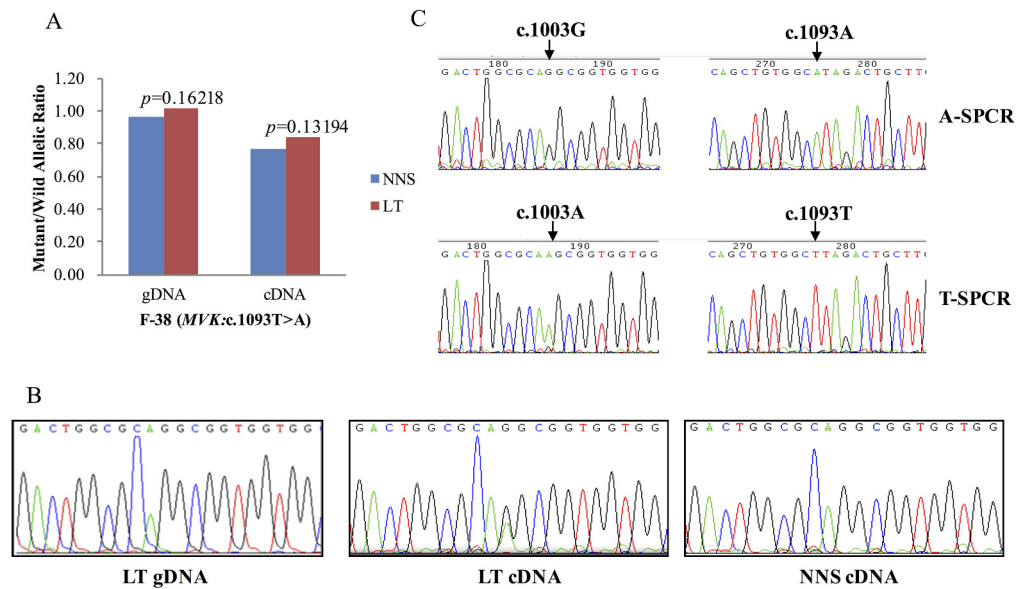


Figure 6. G-to-A RNA editing at position 1003 of the wild allele (T) of c.1093T>A in *MVK* was detected in a left forearm lesion from F-38. **(A)** No allelic expression imbalance was observed in lesional tissue (LT) from F-38. **(B)** A mutation of c.1003G>A was identified in LT cDNA, but not in neighboring normal-appearing skin (NNS) cDNA or LT gDNA. **(C)** Sequencing the c.1093A and c.1093T allele-specific PCR products indicated the mutant allele(A) of c.1003G>A was in the cis position with the wild allele(T) of c.1093T>A. A-SPCR, c.1093A-specific PCR; T-SPCR, c.1093T-specific PCR.

DOI: <http://dx.doi.org/10.7554/eLife.06322.015>

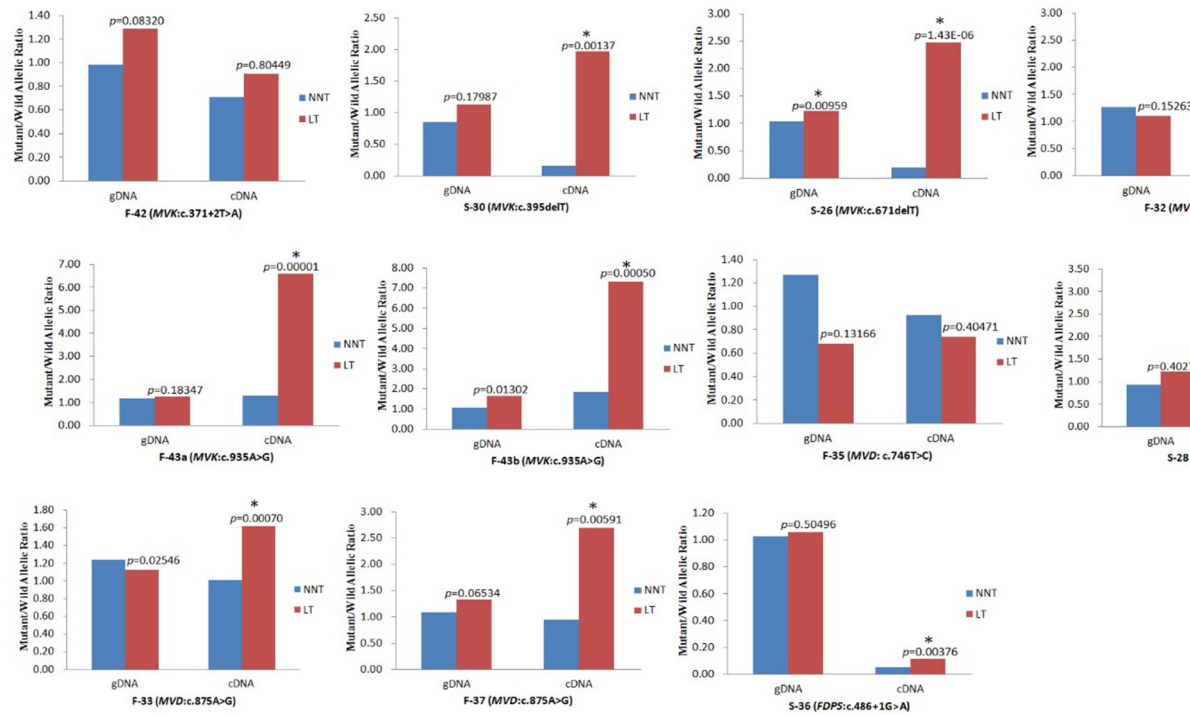


Figure 7. Significantly reduced expression of the wild allele in other nine lesion tissues. The Student t-test was performed to measure the difference in mutant/wild allelic ratios in genomic DNA (gDNA) or complementary DNA (cDNA) from lesion tissue (LT) and neighboring normal-appearing skin (NNS) for each mutation. The test score (p value) is presented above the LT bars. The asterisk (*) designates a significance level of 1%. F-43a and F-43b indicates the tissue sets of the left forearm and left thigh, respectively, from the same F-43 patient.

DOI: <http://dx.doi.org/10.7554/eLife.06322.016>